

# Three-dimensional reconstruction with serial whole-mount sections of oral tongue squamous cell carcinoma: A preliminary study

Yujia Wang<sup>1</sup> | Sheng Chen<sup>1</sup> | Yanhong Ni<sup>1</sup> | Derek Magee<sup>2</sup> | Yumei Pu<sup>1</sup> |  
Qian Zhou<sup>1</sup> | Zhiyong Wang<sup>1</sup> | Lei Zhang<sup>1</sup> | Xiaofeng Huang<sup>1</sup> | Qingang Hu<sup>1</sup> 

<sup>1</sup>Nanjing Stomatological Hospital, Medical School of Nanjing University, Nanjing, China

<sup>2</sup>The School of Computing, University of Leeds, Leeds, UK

## Correspondence

Qingang Hu, Department of Oral and Maxillofacial Surgery, Nanjing Stomatological Hospital, Medical School of Nanjing University, Nanjing, China.  
Email: .qghu@nju.edu.cn  
and

Xiaofeng Huang, Nanjing Stomatological Hospital, Medical School of Nanjing University, Nanjing, China.  
Email: .hxf681008@sina.com

## Funding information

National Key Disciplines Constructional Project Funding, China; Nanjing Municipal Key Medical Laboratory Constructional Project Funding (Since 2012); Center of Nanjing Clinical Medicine Tumor (Since 2014)

**Objectives:** Margin status and invasion pattern are prognostic factors for oral tongue squamous cell carcinoma (OTSCC). Current methods to identify these factors are limited to 2D observation; it is necessary to explore 3D reconstruction with whole-mount sample to improve the accuracy of analysis. This study aimed to study the tissue preparation, section generation, and 3D reconstruction with whole-mount OTSCC specimen.

**Study design:** Two OTSCC samples were retrieved from Nanjing Stomatological Hospital, Medical School of Nanjing University. One sample was sliced into 3 equal-sized pieces and subjected to different processing schedules to determine the best method. The second sample was processed accordingly. Serial whole-mount sections of the second sample were generated, stained with HE/anticytokine antibody in intersection manner, and scanned into digital images. Digital images were aligned and reconstructed into 3D images with Hetero Genius Medical Image Manager 3D Pathology Add-On [HGMIM3D].

**Results:** Successful serial whole-mount sections of comparable quality to traditional sections were generated. Three-dimensional images with serial whole-mount sections were successfully generated.

**Conclusions:** Whole-mount histopathological 3D reconstruction of OTSCC was successfully generated, providing a solid foundation for comprehensive margin and invasion analysis. Although future study and improvement were needed, whole-mount histopathological 3D reconstruction proved to be a promising method in OTSCC study.

## KEYWORDS

invasion, margin status, oral tongue squamous cell carcinoma, serial whole-mount sections, three-dimensional reconstruction

## 1 | INTRODUCTION

Oral tongue squamous cell carcinoma (OTSCC) is the most common form of oral squamous cell carcinoma (OSCC). Many factors influence the prognosis of OTSCC, among which margin status is a

crucial one.<sup>1,2</sup> Despite an overwhelming consensus that failure to eradicate tumor at the primary site is the single largest cause of death for OSCC patients, the present method to access margin status is limited with small samples of limited area.<sup>3</sup>

Margin design is more difficult in deep connective tissue planes as compared to mucosal margins.<sup>3</sup> A clear margin in OTSCC is often described as margins >5 mm away from the invasion front of tumor.<sup>4</sup>

Yujia Wang and Sheng Chen contributed equally to this article.

To better understand the invasion pattern of OTSCC in a more comprehensive way, and to study the relation between invasion front and surgical margin, can provide useful information in margin design.

Invasion pattern has been found to correlate with the prognosis of OTSCC.<sup>5</sup> In 2D observation, pattern of invasion (POI) is examined at the host/tumor interface according to the POI types 1 through 5 previously defined by Bryne et al.<sup>6,7</sup> The highest score of POI presented is taken as the worst pattern of invasion (WPOI), no matter how focal. WPOI is a significant histopathological factor for OSCC prognosis.<sup>5,8</sup> Even though WPOI system is a convenient and valuable assessment in invasion pattern, it has its limitations because of the limited volume of sample. Therefore, 3D investigation is a promising tool for adding up to our knowledge of tumor invasion pattern, and this knowledge can be further applied in margin design.

As a first step, we aim to develop a method to generate a 3D reconstruction with serial whole-mount sections of OTSCC, thus accurate accession could be possible. Detailed experience is shared in this article.

## 2 | METHODS

### 2.1 | Sample collection and tissue preparation

Two OTSCC patients, who went through primary radical resection in the Department of Oral and Maxillofacial Surgery, Nanjing Stomatological Hospital, Medical School of Nanjing University, were included into the study. Ethical approval had previously been obtained from the Nanjing Stomatological Hospital Research Ethics Committee. Written informed consents were obtained from participants prior to delivery.

After resection, the whole-mount sample was fixed with pins to maintain its original form, and fixed in 10% neutral-buffered formalin for 24 hours. After fixation, the whole-mount samples were sliced into 4-mm-thick pieces. The 3 pieces with equal size and thickness of the first sample were subjected to different procedures. The most appropriate procedure was decided (Figure 1, Table 1), and the 4 pieces of the second sample were processed accordingly.

### 2.2 | Serial histology

After the most satisfying procedure was decided, the second whole-mount sample was prepared accordingly. There were four 4-mm-thick pieces in this sample. Each piece was sliced into approximately 700 4- $\mu$ m sections with horizontal sliding microtome (Rem-710; YAMATO, Tokyo, Japan). Combined staining was performed as previously described.<sup>9</sup> Briefly, each section stack was separated into 3 interleaving series, each with approximately 233 sections. Sections were immersed in xylene twice for paraffin removal and rehydrated by decreasing alcohol gradients (100%, 96%, 70% each 5 minutes). The first series were stained with H&E (Figure 2A), and the second series were stained with the anti-CK antibody according to the manufacturer's prescriptions (DAKO, Dako, Denmark) (Figure 2B). The third series were left empty for future staining of other factor of interest.

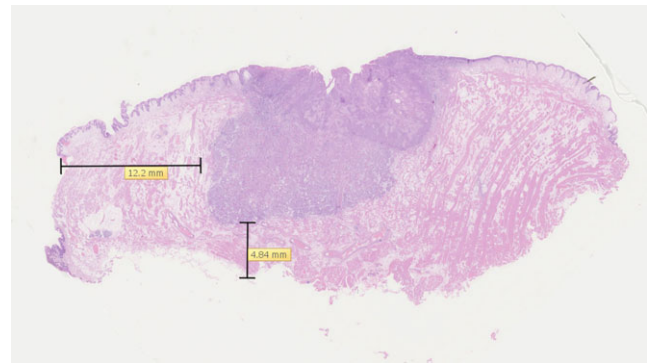


**FIGURE 1** Sections were successfully generated from whole-mount specimen. The whole-mount section revealed a close margin (<5 mm) in the basement that could hardly be recognized with traditional sections

Slides were then imaged using a Hamamatsu Scanner (NanoZoomer-XR C12000, Japan) with a 20 $\times$  objective to produce whole slide images with a final resolution of 0.46  $\mu$ m per pixel. To minimize stain variation, all sections were taken by the same technician on the same microtome and stained in batches. All slides were scanned on the same scanner to minimize interinstrument variation in color.

The HE/CK staining slides were aligned according to their original order (Figure 2C).

### 2.3 | Three-dimensional histological reconstruction

#### 2.3.1 | Auto-alignment

Images of slides were imported into a Windows-based computer in original order. Images with major rotation (rotation > 90 $^\circ$ ) were corrected manually, then images were subjected to auto-alignment by Hetero Genius Medical Image Manager 3D Pathology Add-On [HGMIM3D] (Hetero Genius Ltd, Leeds, UK). During auto-alignment, one representative image (usually high-quality image around the middle of the stack) was manually chosen as reference image, and then, other images were automatically aligned one by one. A stack of 5 images was taken, for example, if Image 3 was chosen as reference, then Image 2 and Image 4 would be automatically aligned with Image 3, after which Image 1 would be aligned with Image 2, and Image 5 with Image 4. During auto-alignment between 2 images, to reduce the computing amount and increase the accuracy, the images were divided into 9 (3  $\times$  3) or more parts depending on the size and outline of images, and each part was aligned with its counterpart in the other image. The auto-alignment could then be checked and improved manually by correcting images with major rotation, redoing auto-alignment among unsatisfyingly aligned images, or increasing the alignment level.

#### 2.3.2 | Volume generation

After images were successfully aligned, volumes could be generated by a simple click of VolumeGenerationMethod. Volume generation could be performed with all images, or selected parts of images. The

**TABLE 1** Paraffin processing schedules: “Routine Tongue” was used for patient care at Nanjing Stomatological Hospital with conventional, small samples, and Schedules A, B, C, and D were compared for large slices

Routines	Routine tongue	A	B	C
Fixation				
10% neutral-buffered formalin	1 h	1 h	1 h	2 h
Dehydration				
50%EtOH	0 h	0 h	8 h	0 h
70%EtOH	1 h	1 h	8 h	2 h
85%EtOH	1 h	1 h	8 h	2 h
95%EtOH	1 h	1 h	8 h	3 h
95%EtOH	1 h	1 h	8 h	3 h
95%EtOH	1 h	1 h	8 h	4 h
100%EtOH	40 min	1.5 h	8 h	4 h
100%EtOH	40 min	1.5 h	8 h	4 h
100%EtOH	40 min	1.5 h	8 h	4 h
Clearing				
Xylene	0.5 h	1 h	4 h	2 h
Xylene	0.5 h	1 h	4 h	2 h
Infiltration				
Paraffin	1 h	1 h	6 h	2 h
Paraffin	1 h	1 h	6 h	3 h
Paraffin	1 h	2 h	6 h	3 h
Heat	No	No	No	Yes, 45°
Dehydration method	MicromSTP120	MicromSTP120	Manual	LEICA ASP 300S

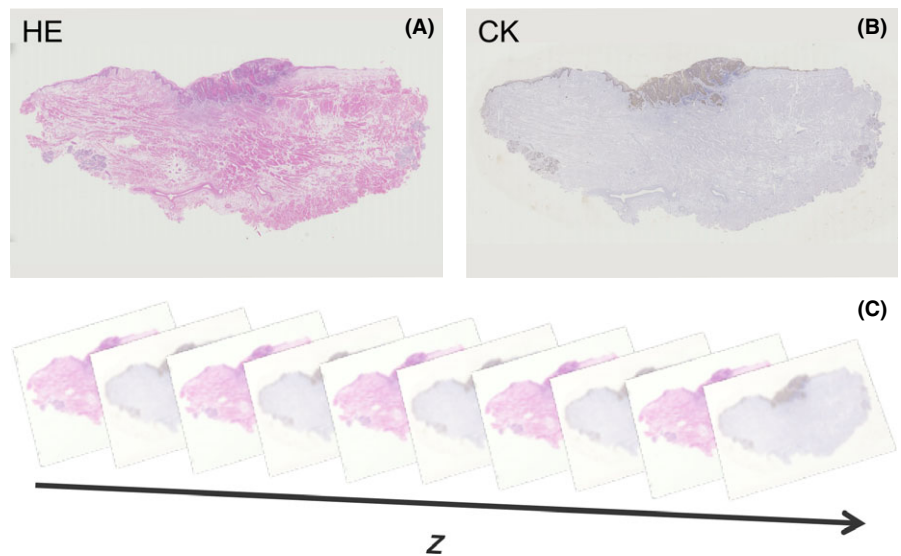


**FIGURE 2** Combined staining with HE/anti-CK. Section stacks were separated into 3 interleaving series. The first series were stained with H&E (A), and the second series were stained with the anti-CK antibody (B). The third series were left empty for future staining of other factor of interest. The HE/CK staining slides were aligned according to their original order, in interleaving way (C)

generated volume could be viewed in whole or in part by adjusting the x-y-z axis settings.

### 2.3.3 | Surface generation

Surface reconstruction provides a better view of items of interests. In CK staining, tumor and epithelium were brown and could be identified by FindTissueByColor algorithm. Auto-annotations could thus be made automatically. Annotations from all images were then

reconstructed into surfaces through SurfaceGeneration algorithm to review tumor and epithelium.

## 3 | RESULTS

### 3.1 | Tissue processing for whole-mount tongue sample

In routine practice at our institution, 4- to 5-mm-thick tongue slices were fixed in 10% NBF for 24 hours, and small samples

(average  $10 \times 20 \times 3 \text{ mm}^3$ ) were processed using the "Routine Tongue" schedule in Table 1. Three promising alternative schedules ("A," "B," and "C") were identified in an attempt to meet the requirements of whole-mount sectioning.

Tissue from each schedule was compared for adequate processing, based on empirical features such as residual xylene odor and ease of sectioning. Sample A appeared to be pale. Complete whole-mount sections could not be generated with sample A, as the tissue was not completely dehydrated. Sample B was overdehydrated. Sections could be made only after softening procedure and with difficulty. Sample C was properly dehydrated and transparent, and was easy to make sections (Figure 1). Both HE staining and immunohistochemistry staining were successfully performed on the whole-mount sections with comparable quality to normal-size sections. It was worth noticing that on the basement of the specimen, which was the primary concern on margin status,<sup>3</sup> the distance between surgical margin and tumor frontier was  $<5 \text{ mm}$  (4.84 mm), while the margin distance to the left was well beyond 5 mm (12.2 mm), confirming the importance of basement margin control and value of whole-mount section in margin observation.

### 3.2 | Auto-alignment and volume reconstruction

To ensure reading speed, images were retrieved from a 1 TB SSD portable hard drive (Samsung, Seoul, Korea). Auto-alignment was based on HGMIM3D AlignAsVolume method using default parameters. Alignment could be performed using 4 increasing levels of magnification (0.3125 $\times$ , 0.625 $\times$ , 1.25 $\times$ , 2.5 $\times$ ), with increasing numbers of B-spline control points used at each level ( $3 \times 3$ ,  $5 \times 5$ ,  $7 \times 7$ ,  $9 \times 9$ ). We performed auto-alignment only on 0.3125 $\times$  as the image size and number were too big. Volumetric data were then generated using the HGMIM3D GenerateVolume method at 0.3125 $\times$  to generate a machine memory fitting volume of approximately  $1000 \times 1000 \times 200$  pixels, suitable for 3D visualization. An image was chosen as the reference image, and the following image was aligned one by one. The alignment result was improved manually and/or by automatic alignment rerun.

As the whole-mount section image was very big, the downsampled version was 3/100 of the original image (20 $\times$  image compressed to 0.6 $\times$ ). When the whole image was compressed to 3/100 of the original image, the compartments such as cancer nest and vessels became very small, and thus hard to align; nonetheless, the

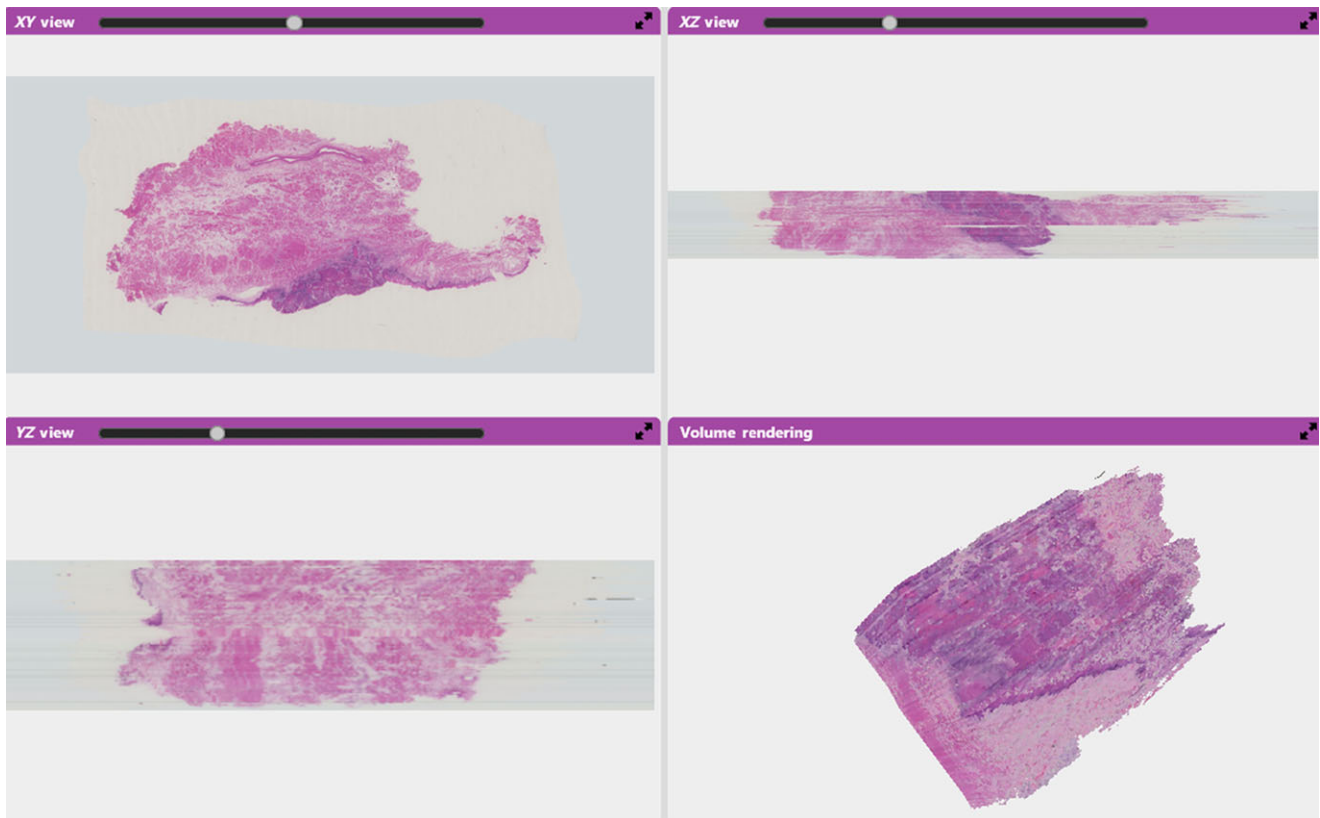


**FIGURE 3** Three-dimensional reconstruction with 2 consecutive pieces with HE staining. Generally, the images were properly aligned inside the same piece. However, a gap could be observed between the 2 sample pieces, indicating that to create a complete consecutive reconstruction image, the target sample should be reconstructed as a whole and should not be separated before sectioning

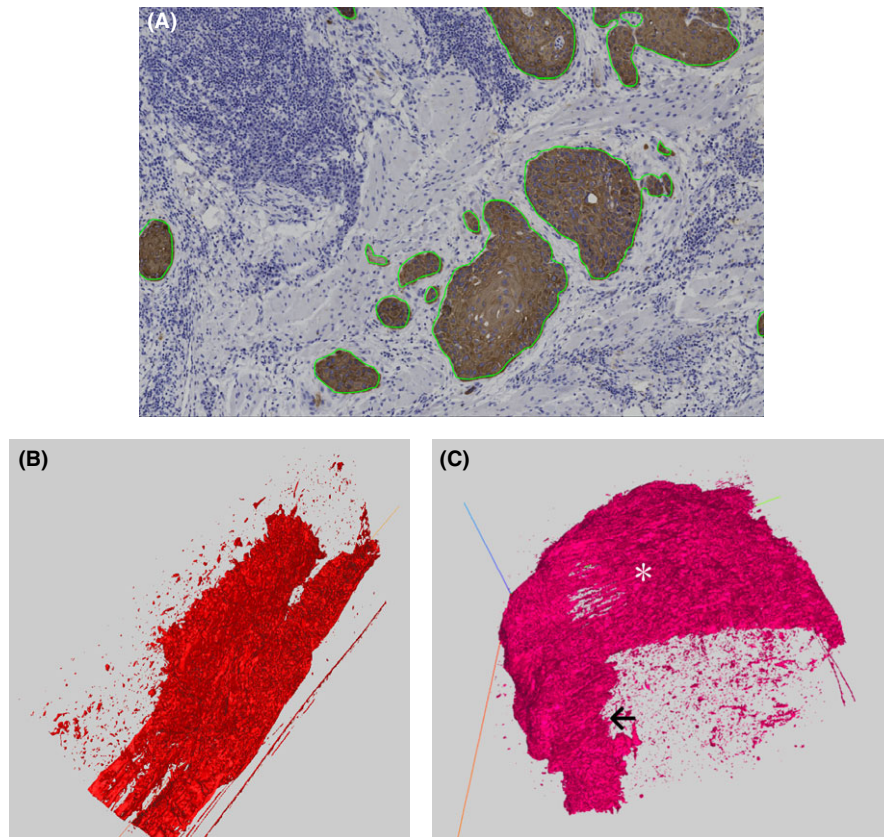


**FIGURE 4** Surface reconstruction with auto-annotations of cancer nests. A, Auto-annotations were successfully generated on CK staining sections, including most of the tumor nests and excluding most of the containments. B, Surface was reconstructed with the annotations on CK staining sections from the 2 sample pieces in the middle, selecting only the cancer parts. C, Surface was reconstructed with the annotations from all 4 sample pieces, shown in half to better visualize the internal structure. \*: tongue back. ←: cancer

general alignment result was satisfying (Figure 3). There was an obvious gap between 2 sample pieces, which was probably caused by the slight rotation on mounting to the slicing machine.

### 3.3 | Auto-annotations and surface reconstruction

For intuitive imaging of specific anatomical features (eg, cancer nest), surface reconstruction could be more informative than simple visualization of the 3D data. Targets could be outlined by annotations either manually or automatically, then the surfaces could be created with annotations to provide three-dimensional image for the item of interest.

As it took much time to annotate manually, CK-positive tissue (cancer and epithelium) was annotated automatically by FindTissueByColor algorithm. Briefly, slides were separated into color blue and color brown, and brown was saved as the auto-annotation result. Different threshold values while generating annotations were tried for different staining.

For CK staining, a threshold of 1000 was most satisfying, which could include most of the cancer nest and exclude most of the non-specific staining (Figure 4A). We generated a 3D triangulated surface from the stack of annotations using the HGMIM3D GenerateSurface method with the annotations for CK staining. The incoherence

mentioned above was more obvious in the reconstructed surface (Figure 4B). Although the annotation threshold excludes most of the non-specific staining, non-specific staining particles could still be observed beyond the invasion front (Figure 4C).

## 4 | DISCUSSION

Margin status and invasion pattern in tumor nest have been proved to be factors of prognostic significance for OTSCC patients.<sup>8,10</sup> As an attempt to develop a method to comprehensively study the margin status and the invasion pattern, we made serial whole-mount sections and performed 3D reconstruction.

First, the most appropriate method to process whole-mount OTSCC specimen was determined. A whole-mount sample was cut into 4-mm-thick pieces of equal size, each subjected to a different process (A, B, and C). A sample was not completely dehydrated, and complete whole-mount section could not be generated. B sample was overdehydrated, and sections could be made only after softening procedure and with difficulty. C sample was properly dehydrated and transparent, and was easy to make sections. The staining quality in both HE staining and immunohistochemistry staining was comparable to their ordinary-size counterparts.

As a novel emerging method, histopathological 3D reconstruction has been applied in the study of cell-cell interaction in cancer,<sup>9</sup> cancer cell invasion, and EMT marker,<sup>11</sup> as well as vessel study.<sup>12,13</sup> As for 3D observation of OTSCC, previous study on invasion front of OTSCC has been limited using limited parts of OTSCC samples,<sup>14</sup> or only microinvasive OTSCC samples.<sup>15</sup> In this study, 3D reconstruction of the whole-mount specimen was successfully generated (Figures 3 and 4).

Still, there were 2 issues worth noticing. First, the specimen was cut into 4 pieces before subjected to sectioning, causing gap in the 3D image that could not be fixed. To generate a complete image without gap, the specimen used should not be cut before sectioning. This, however, leads to another problem, tissue processing. Whole-mount specimen became harder to fixed and dehydrated as it got bigger and thicker. The method we used in this study had not been tested in samples thicker than 5 mm; thus, further study was needed in tissue processing.

Second, as the specimens were all sliced into 4- $\mu$ m-thick sections, adding up to more than 2000 sections in one sample, the workload and cost were considerably high. Two methods might be used to help the problem. First, as it was routine practice that pathologists cut the specimen into pieces, in case of margin assessment, whole-mount section made from each piece could be of help. As described in Result 1, a close margin was found with whole-mount section, which would not be possible with traditional sections. Second, to get a general idea of the 3D margin, not all the successive sections were needed. Mostly using every 10th serial section (~50  $\mu$ m between sections) was sufficient to generate a 3D image.<sup>16</sup> For observation of larger objects, 100  $\mu$ m gap was acceptable (around 100 sections over 1 cm thickness),<sup>17</sup> and thus, the workload could be dramatically reduced.

For margin status study, 3D reconstruction with whole-mount section proved to be a promising tool. As it was advocated that intra-operative resection margin surveillance for en bloc resections should be "specimen driven," rather than "defect driven,"<sup>3</sup> whole-mount section of the specimen, revealing "specimen driven" margins, was bound to provide a more comprehensive assessment of margin status, thus better guiding the resection area. In this study, whole-mount section revealed a close margin (<5 mm) that could otherwise be missed in the basement (Figure 1), further supporting the importance of whole-mount section evaluation and basement margin control. As a preliminary study, we only performed CK immunohistochemistry staining, which only revealed cancer cells and epithelial cells. To better study the surgical margin in terms of "molecular surgical margin," in which the surgical margin status was assessed by the presence of molecular markers rather than solely by histopathologic assessment,<sup>18</sup> more immunohistochemistry staining markers could be added to 3D histopathologic whole-sample reconstruction. It had been shown that molecular alternations in seemingly normal margins were related to poor prognosis.<sup>19</sup> To study the molecular alteration area in 3D prospect, adding different markers that had been prove to be of significance in 2D margin accessions, such as p53, p16, and TMEFF2,<sup>20,21</sup> into the 3D margin

observation, could help us further improve margin design in the future.

For invasion pattern study, we found that if the purpose was only invasion pattern study, to achieve better alignment, whole-mount sections were not necessarily needed. Auto-alignment in HGMIM3D could be performed on 4 increasing levels of magnification (0.3125 $\times$ , 0.625 $\times$ , 1.25 $\times$ , 2.5 $\times$ ), with increasing numbers of B-spline control points used at each level (3  $\times$  3, 5  $\times$  5, 7  $\times$  7, 9  $\times$  9). As the current whole-mount sample was rather big, when aligned on 2.5 $\times$ , the time taken would be 18.2 times that of aligned on 0.3125 $\times$ . When aligned on 0.3125 $\times$  with around 200 whole-mount images, the time was about 6 hours, which would add up to over 2293 hours if we aligned all 2800 images on 2.5 $\times$  with our computer. So it was safe to say that for better alignment to observe smaller structure, such as diffused invasion cancer nests, smaller samples were preferable. Samples, which included all cancerous tissue, should be enough to provide comprehensive invasion pattern information

Three-dimensional reconstruction image with CT and MRI had been applied in surgical design.<sup>22-24</sup> As 3D reconstruction with whole-mount sample could only be obtained after surgery and with considerable amount of time and human work, to use this method to guide margin design before surgery, in future study, we planned to combine whole-mount 3D histopathology reconstruction with CT/MRI reconstruction to access the accuracy of CT/MRI 3D reconstruction compared with whole-mount 3D histopathology reconstruction. In this way, we could better understand the guiding value of CT/MRI 3D reconstruction, thus improving the margin design before surgery.

This preliminary study provided detailed experience in 3D reconstruction of whole-mount sections. The shortcoming of this study was that only 2 samples were used, and thus, further study was needed. Still, whole-mount 3D histopathology reconstruction remained a promising tool in the study of margin status and tumor invasion pattern.

## ACKNOWLEDGEMENTS

We sincerely thank Professor Darren Treanor and Professor Xuebin Yang (both from University of Leeds, Leeds, UK) for their invaluable help in this study. We declare no conflict of interests. This study was supported by the National Key Disciplines Constructional Project Funding, China.

## ORCID

Qingang Hu  <http://orcid.org/0000-0002-5427-3667>

## REFERENCES

1. Jerjes W, Upile T, Petrie A, et al. Clinicopathological parameters, recurrence, locoregional and distant metastasis in 115 T1-T2 oral squamous cell carcinoma patients. *Head Neck Oncol*. 2010;2:9.

2. Meier JD, Oliver DA, Varvares MA. Surgical margin determination in head and neck oncology: current clinical practice. The results of an International American Head and Neck Society Member Survey. *Head Neck*. 2005;27:952-958.
3. Hinni ML, Ferlito A, Brandwein-Gensler MS, et al. Surgical margins in head and neck cancer: a contemporary review. *Head Neck*. 2013;35:1362-1370.
4. Anderson CR, Sisson K, Moncrieff M. A meta-analysis of margin size and local recurrence in oral squamous cell carcinoma. *Oral Oncol*. 2015;51:464-469.
5. Almangush A, Bello IO, Keski-Santti H, et al. Depth of invasion, tumor budding, and worst pattern of invasion: prognostic indicators in early-stage oral tongue cancer. *Head Neck*. 2014;36:811-818.
6. Bryne M, Jenssen N, Boysen M. Histological grading in the deep invasive front of T1 and T2 glottic squamous-cell carcinomas has high prognostic value. *Virchows Arch*. 1995;427:277-281.
7. Brandwein-Gensler M, Teixeira MS, Lewis CM, et al. Oral squamous cell carcinoma: histologic risk assessment, but not margin status, is strongly predictive of local disease-free and overall survival. *Am J Surg Pathol*. 2005;29:167-178.
8. Almangush A, Bello IO, Coletta RD, et al. For early-stage oral tongue cancer, depth of invasion and worst pattern of invasion are the strongest pathological predictors for locoregional recurrence and mortality. *Virchows Arch*. 2015;467:39-46.
9. Wentzensen N, Braumann UD, Einenkel J, et al. Combined serial section-based 3D reconstruction of cervical carcinoma invasion using H&E/p16INK4a/CD3 alternate staining. *Cytometry A*. 2007;71:327-333.
10. Pu Y, Wang Y, Huang X, et al. The influence of mild dysplasia at the surgical margin on the prognosis of oral squamous cell carcinoma. *Int J Oral Maxillofac Surg*. 2016;45:1372-1377.
11. Bronsert P, Enderle-Ammour K, Bader M, et al. Cancer cell invasion and EMT marker expression: a three-dimensional study of the human cancer-host interface. *J Pathol*. 2014;234:410-422.
12. Wang G, Zhong J, Li J, et al. Computer-aided three-dimensional reconstruction of main vessels in hemangiomas. *Int J Clin Exp Med*. 2015;8:1747-1754.
13. Liang Y, Wang F, Treanor D, et al. A framework for 3D vessel analysis using whole slide images of liver tissue sections. *Int J Comput Biol Drug Des*. 2016;9:102-119.
14. Kudo T, Shimazu Y, Yagishita H, et al. Three-dimensional reconstruction of oral tongue squamous cell carcinoma at invasion front. *Int J Dent*. 2013;2013:482765.
15. Amit-Byatnal A, Natarajan J, Shenoy S, Kamath A, Hunter K, Radhakrishnan R. A 3 dimensional assessment of the depth of tumor invasion in microinvasive tongue squamous cell carcinoma—a case series analysis. *Med Oral Patol Oral Cir Bucal* 2015;20:e645-e650.
16. Roberts N, Magee D, Song Y, et al. Toward routine use of 3D histopathology as a research tool. *Am J Pathol*. 2012;180:1835-1842.
17. Magee D, Song Y, Gilbert S, et al. Histopathology in 3D: from three-dimensional reconstruction to multi-stain and multi-modal analysis. *J Pathol Inform*. 2015;6:6.
18. Mao L, Clark D. Molecular margin of surgical resections—where do we go from here? *Cancer*. 2015;121:1914-1916.
19. Stransky N, Egloff AM, Tward AD, et al. The mutational landscape of head and neck squamous cell carcinoma. *Science*. 2011;333:1157-1160.
20. Shaw RJ, Hobkirk AJ, Nikolaidis G, et al. Molecular staging of surgical margins in oral squamous cell carcinoma using promoter methylation of p16(INK4A), cytoglobin, E-cadherin, and TMEFF2. *Ann Surg Oncol*. 2013;20:2796-2802.
21. Dissanayaka WL, Pitiyage G, Kumarasiri PV, Liyanage RL, Dias KD, Tilakaratne WM. Clinical and histopathologic parameters in survival of oral squamous cell carcinoma. *Oral Surg Oral Med Oral Pathol Oral Radiol*. 2012;113:518-525.
22. Fukuda H, Numata K, Nozaki A, et al. Usefulness of US-CT 3D dual imaging for the planning and monitoring of hepatocellular carcinoma treatment using HIFU. *Eur J Radiol*. 2011;80:e306-e310.
23. Wang Y, Sun G, Lu M, Hu Q. Surgical management of maxillofacial fibrous dysplasia under navigational guidance. *Br J Oral Maxillofac Surg*. 2015;53:336-341.
24. Nimeskern L, Feldmann EM, Kuo W, et al. Magnetic resonance imaging of the ear for patient-specific reconstructive surgery. *PLoS One*. 2014;9:e104975.

**How to cite this article:** Wang Y, Chen S, Ni Y, et al. Three-dimensional reconstruction with serial whole-mount sections of oral tongue squamous cell carcinoma: A preliminary study. *J Oral Pathol Med*. 2018;47:53–59. <https://doi.org/10.1111/jop.12644>